Supporting Information

Wu et al. 10.1073/pnas.0806422106

SI Materials and Methods

AC3-I and AC3-C Mice. The AC3-I and AC3-C mice were generated by synthesis of a minigene based on the peptide sequence of AC3-I (KKALHRQEAVDCL) or AC3-C (KKALHAQERVDCL). The engineering and characterization of these mice was previously described (9). Adult mice (2–3 months old) of either gender were used in the experiments. Wild-type (WT) littermate mice also used as a control for potential GFP effects in AC3-C or AC3-I mice. The investigation conforms to the Guide for the Care and Use of Laboratory Animals published by the U.S. National Institutes of Health (NIH Publication No. 85–23, revised 1996).

SAN Cell Isolation and Electrophysiology. Isolation of single SAN cells from mice was performed as a modified method based on DiFrancesco et al. (1), and Mangoni and Nargeot (2). Mice were administered an i.p. injection of heparin (1,000 units/mL) and Avertin (20 μL/g). The heart was excised and placed into Tyrode's solution (35 °C), consisting of (mM) 140 NaCl, 5.0 Hepes, 5.5 Glucose, 5.4 KCl, 1.8 $CaCl_2$, 1.0 $MgCl_2$, with pH adjusted to 7.4 with NaOH. The SAN region, delimited by the crista terminalis, atrial septum, and orifice of superior vena cava, was dissected from the heart. The SAN was cut into smaller pieces, which were transferred and rinsed in a "low Ca^{2+}" solution containing (mM) 140 NaCl, 5.0 Hepes, 5.5 Glucose, 5.4 KCl, 0.2 $CaCl_2$, 0.5 $MgCl_2$, 1.2 KH_2PO_4, 50 Taurine, and 1 mg/mL BSA with pH adjusted to 6.9 with NaOH. SAN tissue pieces were digested in 5 mL of "low Ca^{2+}" solution containing collagenase type I, elastase (Worthington), and protease type XIV (Sigma) for 20 to 30 min. Then the tissue was transferred to 10 mL of Kraft-Bruhe medium containing (mM) 100 potassium glutamate, 5.0 Hepes, 20 Glucose, 25 KCl, 10 potassium aspartate, 2.0 $MgSO_4$, 10 KH_2PO_4, 20 taurine, 5 creatine, 0.5 EGTA, and 1 mg/mL BSA, with pH adjusted to 7.2 with KOH. The tissue was agitated using a glass pipette for 10 min. The cells were stored at 4 °C and studied within 7 hr.

SAN cells were placed in Tyrode's solution at 36 ± 1 °C. SAN cells were identified by their characteristic morphology (spindle or spider shape) and spontaneous activity. SAN cells were identified electrophysiologically by typical spontaneous action potentials with slow depolarizing phase 4 and the hyperpolarization-activated current I_f.

Spontaneous action potentials (APs) were recorded using the perforated (amphotericin B) patch-clamp technique (3) on single SAN cells at 36 ± 1 °C in Tyrode's solution with the pipette filled with (mM) 130 potassium aspartate, 10 NaCl, 10 Hepes, 0.04 $CaCl_2$, 2.0 MgATP, 7.0 phosphocreatine, 0.1 NaGTP, and amphotericin B 240 μg/mL, with the pH adjusted to 7.2 with KOH. SAN cells with stable APs were included in the experiments.

I_f was recorded using the whole-cell patch-clamp technique at 36 ± 1 °C as described (4). Patch pipettes had a resistance of 3 to 5 MΩ when filled with intracellular solution, containing (mM): 120 potassium aspartate, 25 KCl, 4.0 $MgCl_2$, 10 EGTA, 4.0 KATP, 2.0 NaGTP, 2.0 phosphocreatine, 5.0 Hepes, and 1.0 $CaCl_2$, and the pH was adjusted to 7.2 with KOH. The extracellular solution contained (mM): 130 NaCl, 5.0 KCl, 2.0 $MgCl_2$, 1.8 $CaCl_2$, and 5.0 Hepes; the pH was adjusted to 7.4 with NaOH. After the initial current recordings, 0.5 mM $BaCl_2$ was applied to extract the Ba^{2+}-sensitive potassium component. The conditioning voltage steps were applied for 1.0 sec ranging from −120 mV to −50 mV in 10 mV increments.

I_{Ca} was measured using perforated patch technique (3) at 36 ± 1 °C. I_{Ca} was confirmed by its sensitivity to Nifedipine 5 μM. Depolarizing voltage pulses (300 ms in duration) to various potentials (−60 mV to 60 mV in 10 mV steps) were applied from a holding potential of −70 mV. The pipette (intracellular) solution comprised (mM): 120 CsCl, 10 EGTA, 10 Hepes, 10 tetraethylammonium chloride (TEA), 5.0 phosphocreatine, 3.0 $CaCl_2$, 1.0 MgATP, and 1.0 NaGTP; the pH was adjusted to 7.2 with 1.0 N CsOH. The bath (extracellular) solution comprised (mM): 137 NaCl, 10 Hepes, 10 glucose, 1.8 $CaCl_2$, 0.5 $MgCl_2$, and 25 CsCl; pH was adjusted to 7.4 with NaOH.

I_{NCX} was recorded as described (5). Briefly, whole-cell recordings were obtained at 36 ± 1 °C with the use of standard patch-clamp techniques. The electrode resistance ranged from 2 to 4 MΩ. The external solution contained the following (mM): 145 NaCl, 1.0 $MgCl_2$, 5.0 Hepes, 2.0 $CaCl_2$, 5.0 CsCl, and 10 glucose (pH 7.4, adjusted with NaOH). The internal solution contained the following (mM): 65 CsCl, 20 NaCl, 5.0 Na_2ATP, 6.0 $CaCl_2$, 4.0 $MgCl_2$, 10 Hepes, and 20 tetraethyl ammonium chloride, 21 EGTA (pH 7.2, adjusted with CsOH). Membrane currents were elicited by command ramps. The protocol was applied every 12 sec. I_{NCX} was measured as the Ni-sensitive current. Ni^{2+} (5 mM) was added to define the fraction of current from NCX (the difference between total current and post-Ni^{2+} current).

Electrocardiographic Telemetry. Surgical implantation of ECG telemeters was performed as described (6). Mice are anesthetized with ketamine/xylazine (87.5/12.5 mg/kg), and an ECG transmitter (DSI model Ta10EA-F20) is implanted in the abdominal cavity. The leads are placed s.c. in a lead I configuration. After a 5-day recovery period, experiments begin. Continuous recordings are performed for 30 min intervals to establish baseline. After 30 min, the recording is briefly interrupted, during which time an injection is given. After injections are completed (≈1min), recordings are continued for 30 additional min.

Measurement of Catecholamines in Mouse Plasma. Catechols in mouse samples were absorbed onto acid washed alumina (20 mg) at pH 8.6, washed, and eluted with dilute acid. After microfiltration, the eluate was further diluted in 4% acetic acid and the chromatographic resolution of catecholamines was achieved using an Aquasil C18 4 μm (100 × 4.6 mm) HPLC column (Thermo Electron Corp.). Catecholamines were subsequently analyzed by electrochemical detection (Coulochem II Dual Potentiostat EC Detector, ESA). Plasma extract peak areas for norepinephrine, epinephrine, and dopamine were compared with the average peak areas determined from the injection of 100 pg pure standard. Results were corrected for extract dilutions and original plasma volume with final concentrations expressed as picograms per milligram.

Viral Infection with CaMKIIN/eGFP. Freshly isolated mice SAN pacemaker cells were allowed to settle onto laminin-coated coverslips in 35 mm tissue culture plates. These cells were cultured for 2 hr in RPMI medium 1640 (Invitrogen) for cell attachment. Fresh medium (RPMI medium 1640) containing Ad-eGFP or Ad-CaMKIIN was added to the plates at a multiplicity of infection of 100. Ad-CaMKIIN (expressing CaMKIIN) (7) and Ad-eGFP were generated as follows: CaMKIIN cDNA was cloned into the pCMV-HA vector (Clontech). HA-

CAMKIIN cDNA was inserted into the adenoviral shuttle vector pacAd5 CMV IRES eGFP pA using the BamH1 and EcoR1 restriction sites. (Adenovirus recombination and amplification was performed by the Gene Transfer Vector Core at the University of Iowa.). Expression of the recombinant CaMKIIN in SAN cells was detected by GFP. Recombinant adenovirus that expresses eGFP only (Ad-eGFP) was used as a control.

Immunofluorescence Studies. Isolated mouse SAN cells were gently washed with PBS (PBS, pH 7.4) and immediately fixed in 2% paraformaldehyde for 20 min. Cells were blocked/permeabilized in PBS containing 0.075% Triton X-100, 2 mg/mL BSA, and 3% fish gelatin and incubated in primary antibody overnight at 4 °C. Following PBS washes, cells were incubated in secondary antibody (Alexa 568; 633; Molecular Probes) for 2 hr at room temperature and mounted using Vectashield (Vector) and #1 coverslips. Images were collected on a Zeiss 510 Meta confocal microscope (63 power oil 1.40 NA [Zeiss], pinhole equals 1.0 Airy Disc) using Carl Zeiss imaging software. Images were imported into Adobe Photoshop for cropping and linear contrast adjustment.

PLN Immunodetection Studies. Western analyses were performed to monitor the phosphorylated (phosphor-serine S16 and phosphor-threonine T17) and native PLN expression in SAN tissue explants isolated from WT as well as AC3-I and AC3-C transgenic mice. SAN extracts were prepared in an extraction buffer (50 mM Hepes, pH 7.5; 150 mM NaCl; 1% vol/vol Nonidet P-40; 0.5% sodium deoxycholate; and 5 mM EDTA) with protease and phosphatase inhibitors. Protein extracts (10 μg total protein/lane) were fractionated on bis-Tris NuPAGE gels (Invitrogen) with 1x Mops-SDS running buffer and transferred to PVDF membrane (Bio-Rad). After blocking the nonspecific binding by 10% nonfat powdered milk in TBS-T (50 mM Tris-HCl, pH 7.6, 150 mM NaCl, and 0.05% Tween 20), membranes were incubated either with anti-phospho-Ser-16 or anti-phospho-Thr-17 antibodies (both antibodies raised in rabbit, Cyclacell, U.K.). After washing, the membranes were incubated with horseradish peroxidase (HRP)-conjugated secondary antibodies (Amersham). Signals from bound antibodies were visualized by using the enhanced chemiluminescence detection system (Roche). Blots were then stripped of the antibodies at 55 °C in a buffer containing 2% (wt/vol) SDS, 62.5 mM Tris·HCl (pH 6.8), and 100 mM β-ME; rinsed in TBS-T; and probed again for native phospholamban using mouse monoclonal antibody (Cyclacell, U.K.) as described above except an HRP-conjugated anti-mouse secondary antibody was used. Levels of total PLN, PLN-phospho-Ser-16, and PLN-phospho-Thr-17 were quantified by scanning the ECL signals and quantifying using QuantityOne software (Bio-Rad). Subsequently, averaged data were calculated for each condition and antibody, and ratios of PLN-pThr17/ total PLN, and PLN-pSer16/ total PLN signals were calculated.

PKA Activity. PKA activity was determined by transfer of radioactive PO_4^- to protein kinase A substrate Kemptide using a commercial kit according to the suggested protocol (Upstate, NY). SA nodal tissue samples were surgically removed from ISO treated mice and immediately frozen in liquid nitrogen. Tissue samples were homogenized in a buffer containing 25 mM Tris, pH 7; 5 mM EDTA, 10 mM EGTA; 1 mM DTT; 1 mM sodium orthovanadate, and 1 mM PMSF. Protein kinase activity in each tissue homogenate was determined in a 60 μl reaction volume in the presence of [γ-^{32}P]ATP and PKC- and CaM kinase-inhibitors, and the specificity of PKA activity was confirmed by addition of PKA inhibitor peptide. Incorporation of radionuclide in substrate Kemptide was monitored by adsorbing the Kemptide onto P81 phosphocellulose filter paper followed by scintillation counting. Control reactions without the addition of homogenate were used as background controls.

Myristoylated Peptides. Myristoylated-AIP CaM Kinase II inhibitor (Biomol International, Inc.) 10 μM or myristoylated-AC3-C (as a control, synthesized by ANASPEC) 10 μM in bath solution was applied to SAN cells.

Langendorff Perfusion. ECG recording from Langendorff-perfused hearts was performed as described (8). Briefly, excised hearts were quickly mounted on a modified Langendorff apparatus (HSE-HA perfusion systems, Harvard Apparatus) for retrograde aortic perfusion at a constant pressure of 80 mm Hg with oxygenated (95% O_2, 5% CO_2) Krebs-Henseleit solution consisting of (mM) 25 $NaHCO_3$, 118 NaCl, 4.7 KCl, 1.2 $MgSO_4$, 1.2 NaH_2PO_4, 2.5 $CaCl_2$, 0.5 Na-EDTA, and 15 glucose, with pH equilibrated to 7.4. The perfused heart was immersed in the water-jacked bath and was maintained at 36 °C. ECG of the intact heart was continuously recorded with Ag^+-AgCl electrodes, which were positioned around the heart in an approximate Einthoven configuration. After the heart was allowed to stabilize for 15 min, different concentrations of isoproterenol were perfused (5 min). For some studies, the hearts were perfused with 5 μM H89 (Sigma), a PKA inhibitor, for 20 min, followed by 100 nM isoproterenol in the continued presence of H-89 by a further 5 min.

SR Ca^{2+} Content Measurements. SR Ca^{2+} content of SAN cells was measured by integrating the I_{NCX} in response to a "spritz" of caffeine (9). Briefly, cells were held at −80 mV for >5 min for adequate dialysis with pipette solutions before initiating experiments. Cells were loaded with Ca^{2+} by stepping the cell membrane from −80 to 0 mV with a duration of 300 ms at 0.5 Hz (36 ± 1 °C). The bath solution contained (mM): 137 NaCl, 10 Hepes, 10 glucose, 1.8 $CaCl_2$, 0.5 $MgCl_2$, and 25 CsCl; pH was adjusted to 7.4 with NaOH. The intracellular pipette solution contained (mM): 120 CsCl, 10 TEA, 1.0 MgATP, 1.0 NaGTP, 5.0 phosphocreatine, 10 Hepes, and Indo-1 0.2, and the pH was adjusted to 7.2 with 1.0 N CsOH. Voltage-activated Na^+ current was inactivated by a 50 ms depolarization step to −40 mV before completing the depolarization to 0 mV. The K^+ currents were eliminated by adding Cs^+ and TEA and omitting K^+ from the pipette and bath solutions. After loading Ca_i^{2+} with >15 conditioning command steps, caffeine 20 mM was locally applied by a pipette close to the cell of study (DAD-12 Superfusion System, ALA Scientific Instruments) while the cell was holding at −80 mV. The Na^+/Ca^{2+} exchanger currents induced by caffeine were integrated and normalized to cell size.

Intracellular Ca^{2+} Transients and Sparks. Single isolated SAN cells were loaded with 5 μM Rhod-2 acetoxymethyl ester for 10 min, and then rested for 20 min for deesterization in normal Tyrode's solution. After placement on a recording chamber, the cells were perfused in normal Tyrode's solution at 36 °C ± 1 (Temperature Controller, TC2BIP, Cell MicroControls). Spindle-shaped, active spontaneously beating cells were chosen for experiments. Confocal Ca^{2+} imaging was performed in line scan mode at a speed of 1.92 ms per line. The scan lines were scanned along the cell edge because Ca^{2+} release occurs mostly in the SAN cell periphery. In some experiments, action potential recording (Axon 200B, Molecular Devices) and confocal Ca^{2+} imaging (LSM510, Carl Zeiss MicroImaging) were performed simultaneously. The synchronization between confocal Ca^{2+} signals and electrical activities was achieved by an internal triggering signal sent from confocal imaging software. Analysis of Ca^{2+} transients and sparks was performed offline with IDL program (Research System Inc.), as we described previously (10).

1. DiFrancesco D, Ferroni A, Mazzanti M, Tromba C (1986) Properties of the hyperpolarizing-activated current (I_f) in cells isolated from the rabbit sino-atrial node. *J Physiol* 377:61–88.
2. Mangoni ME, Nargeot J (2001) Properties of the hyperpolarization-activated current (I_f) in isolated mouse sino-atrial cells. *Cardiovasc Res* 52:51–64.
3. Rae J, Cooper K, Gates P, Watsky M (1991) Low access resistance perforated patch recordings using amphotericin B. *J Neurosci Methods* 37:15–26.
4. Cho HS, Takano M, Noma A (2003) The electrophysiological properties of spontaneously beating pacemaker cells isolated from mouse sinoatrial node. *J Physiol* 550:169–180.
5. Wei SK, et al. (2007) Muscarinic modulation of the sodium-calcium exchanger in heart failure. *Circulation* 115:1225–1233.6.
6. Wu Y, et al. (2002) Calmodulin kinase II and arrhythmias in a mouse model of cardiac hypertrophy. *Circulation* 106:1288–1293.
7. Chang BH, Mukherji S, Soderling TR (1998) Characterization of a calmodulin kinase II inhibitor protein in brain. *Proc Natl Acad Sci USA* 95:10890–10895.
8. Li J, et al. (2006) Calmodulin kinase II inhibition shortens action potential duration by upregulation of K^+ currents. *Circ Res* 99:1092–1099.
9. Zhang R, et al. (2005) Calmodulin kinase II inhibition protects against structural heart disease. *Nat Med* 11:409–417.
10. Song LS, et al. (2006) Orphaned ryanodine receptors in the failing heart. *Proc Natl Acad Sci USA* 103:4305–4310.

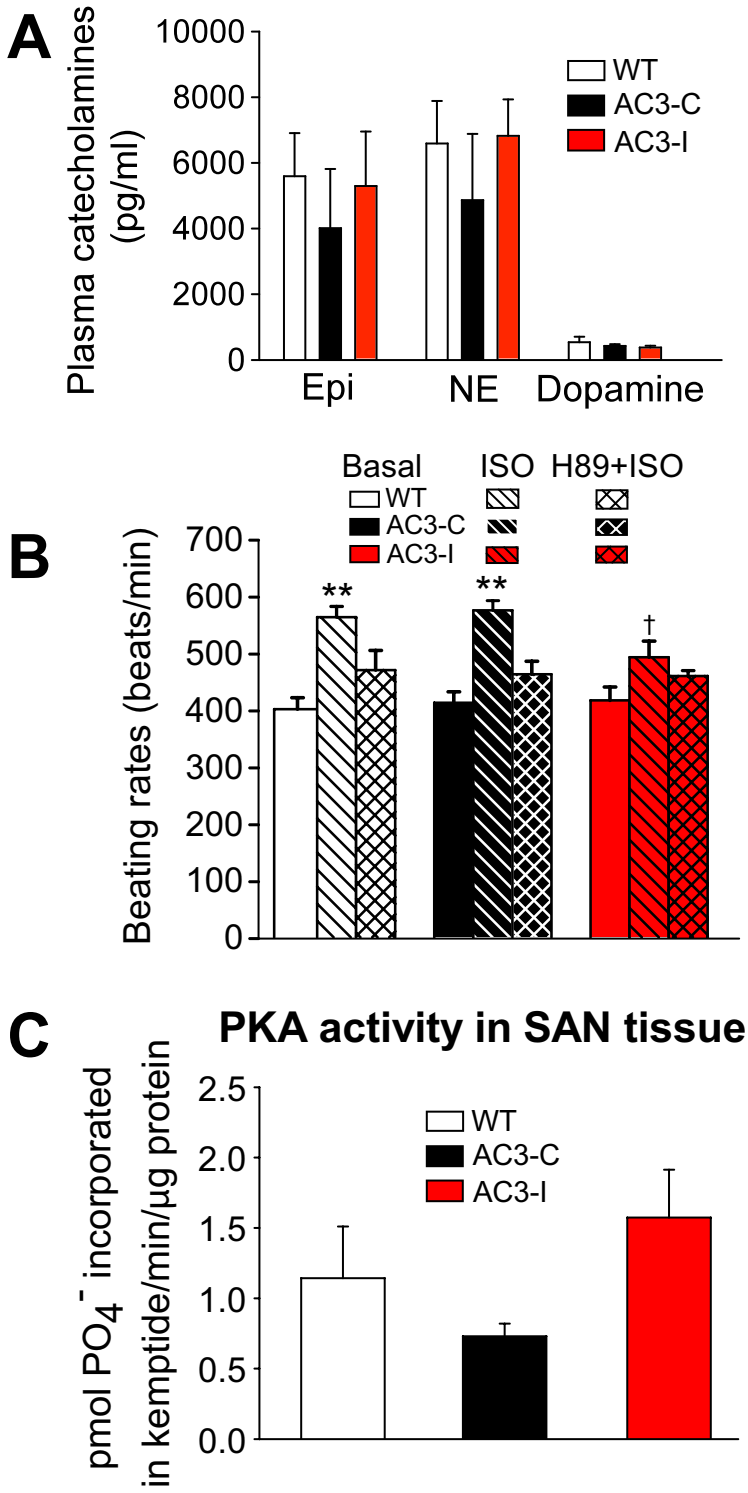

Fig. S1. Plasma catecholamines and PKA responses to catecholamine stimulation. (*A*) Equivalent plasma catecholamines in AC3-I, AC3-C, and WT mice. Summary data are from 3 to 4 mice/group. There were no significant differences in epinephrine (Epi), norepinephrine (NE), or dopamine concentrations between genotypes. (*B*) H89 (5 μM) causes similar reduction in ISO (100 nM) stimulated rates in Langendorff-perfused hearts from AC3-I, AC3-C, and WT mice. AC3-I rates were significantly slower than AC3-C and WT hearts after ISO (†, $P<0.05$), but this difference was eliminated by H89 treatment ($P = 0.959$). **, $P<0.01$ compared with baseline. Data represent 5 to 6 hearts per group. (*C*) No significant differences in PKA activity from SAN explants after ISO injection (0.4 mg/kg) between genotypes ($P = 0.3$). Each data bar represents 3 to 4 studies.

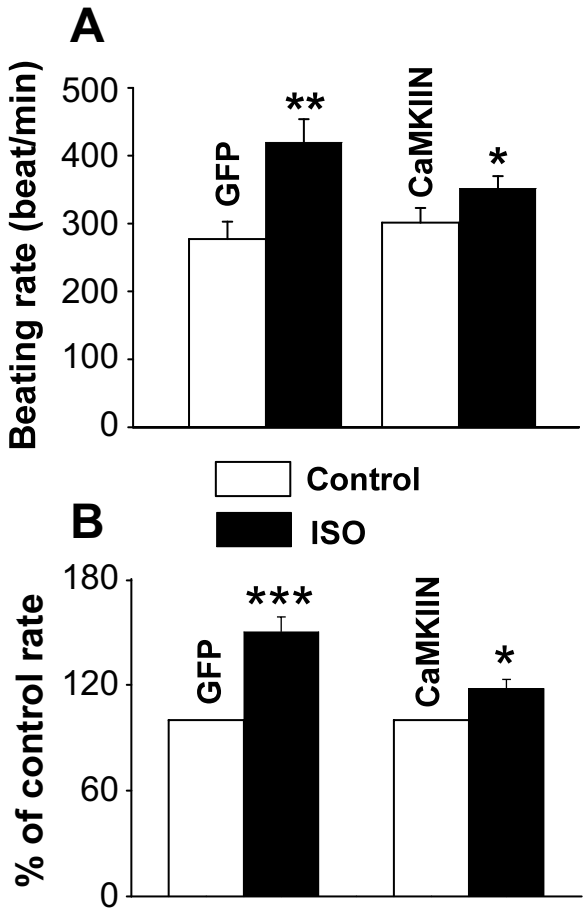

Fig. S2. Short-term (24 hr) CaMKII inhibition by the CaMKII inhibitory peptide CaMKIIN phenocopies chronic AC3-I expression. (*A*) Action potential frequencies in WT SAN cells infected with adenovirus encoding eGFP alone or eGFP+CaMKIIN. (*B*) Data are normalized to baseline, $n = 5–7$/group. ***, $P < 0.001$, **, $P < 0.01$, and *, $P < 0.05$ compared with baseline.

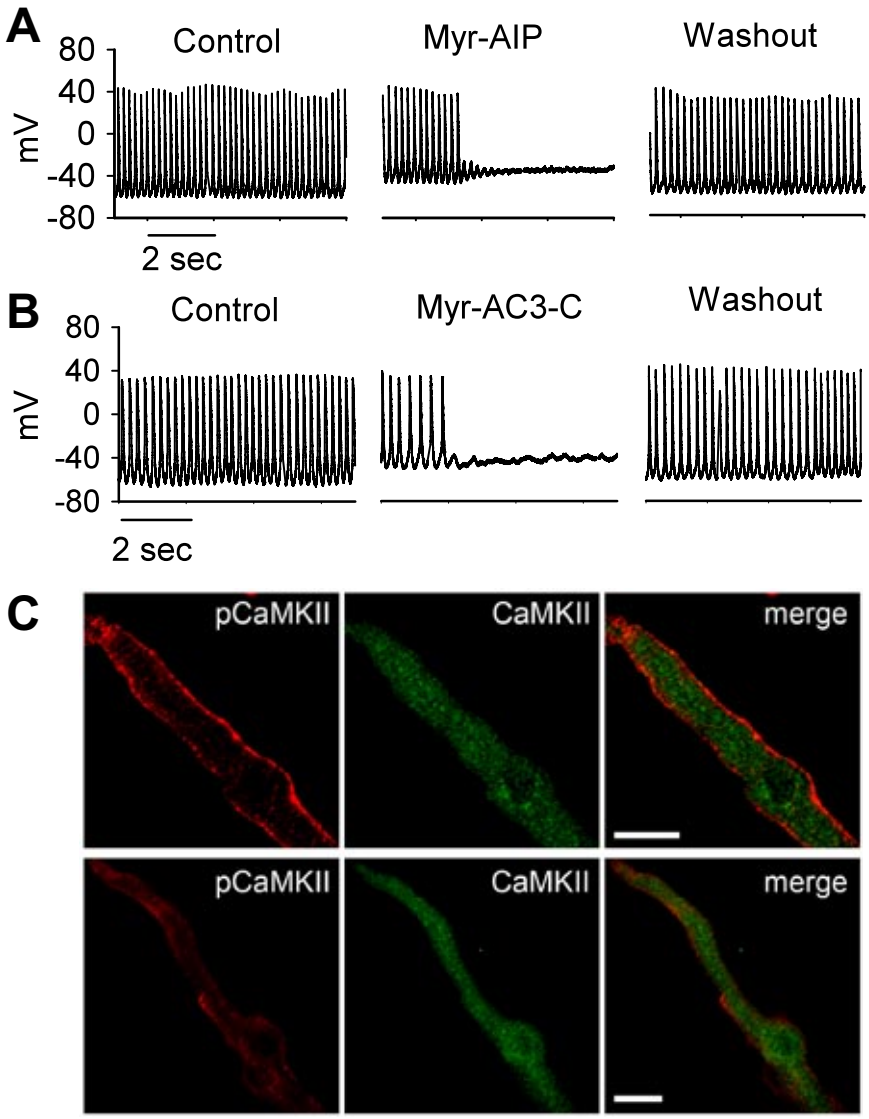

Fig. S3. Representative tracings showing the effects of cell membrane permeant peptides on SAN automaticity in WT SAN cells. (*A*) CaMKII inhibitory peptides (Myr-AIP) and (*B*) Myristoylated control (Myr-AC3-C) eliminate spontaneous SAN automaticity at a low (10 μM) concentration. The effects of these myristoylated peptides are reversible by wash out. (*C*) Representative immunofluorescence micrographs of WT SAN cells treated with Myr-AC3-C (*Upper*) or Myr-AIP (*Lower*) and ISO (1 μM). ISO activates CaMKII more in SAN cells treated with Myr-AC3-C than in Myr-AIP treated cells (both peptides 100 μM), as evidenced by immunodetection of Thr 287 autophosphorylated CaMKII (pCaMKII, red, *Left*). Total CaMKII expression is similar in Myr-AC3-C and Myr-AIP treated SAN cells (green, *Center*). Autophosphorylated and total CaMKII images are merged (*Right*). (Scale bar, 10 μm.)

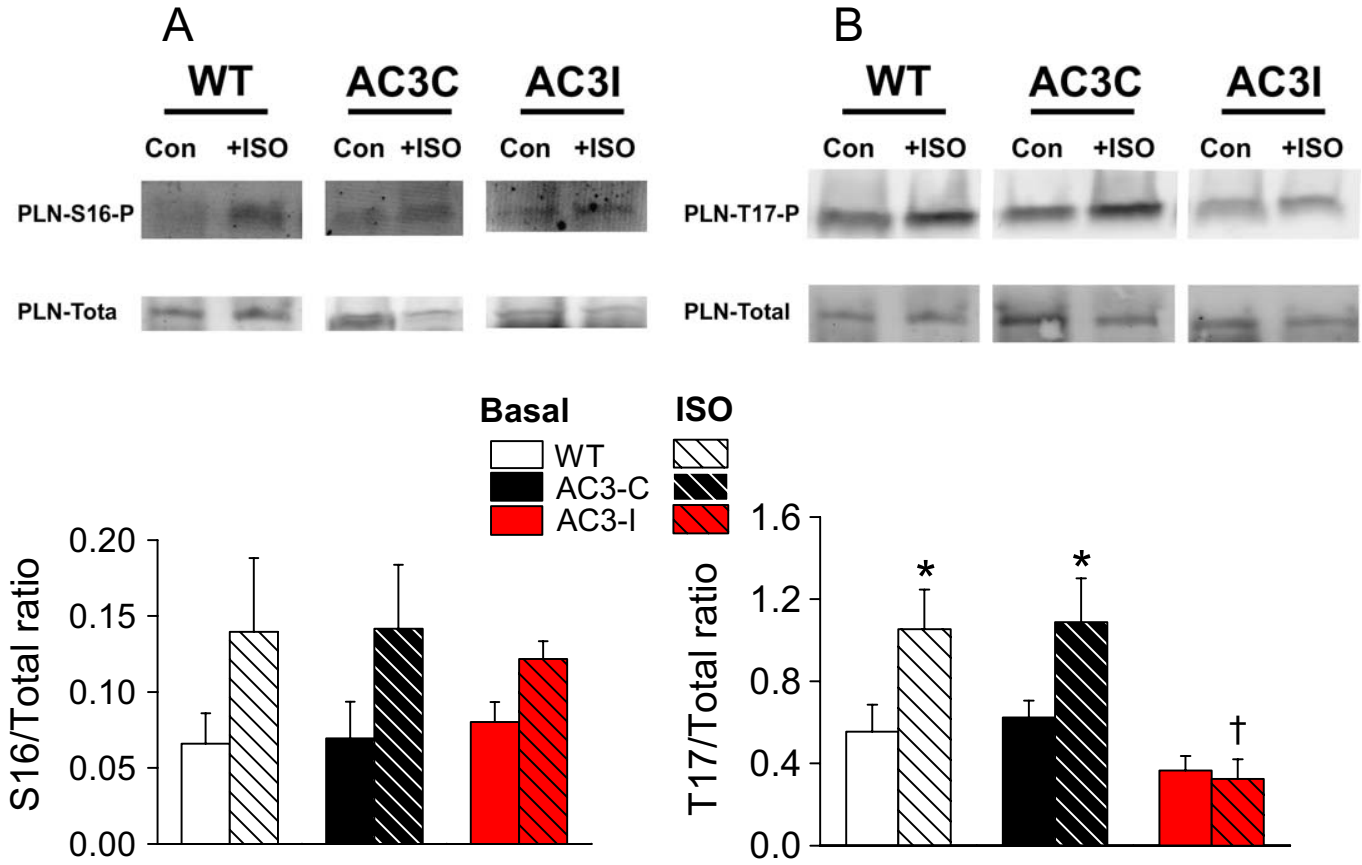

Fig. S4. Reduced CaMKII activity and no change in PKA activity at PLN in AC3-I SAN. (*A*) Western blots and summary data from SAN tissue explants are treated with ISO (1 μM) for 30 min and probed with phosphor-specific antibodies against PLN Ser-16. All genotypes show an increase in PLN Ser 16 phosphorylation after ISO. There are no significant differences in basal or ISO stimulated PLN Ser-16 phosphorylation between genotypes. (*B*) Western blots and summary data from SAN tissue explants are treated with ISO (1 μM) for 30 min and probed with phosphor-specific antibodies against PLN Thr-17. Thr-17 phosphorylation was significantly reduced in AC3-I SAN explants compared with controls after ISO; †, $P < 0.05$ compared with both control groups (ANOVA). ⋆, $P < 0.05$ after ISO versus baseline in each group. The summary data were from 5 mice per group.

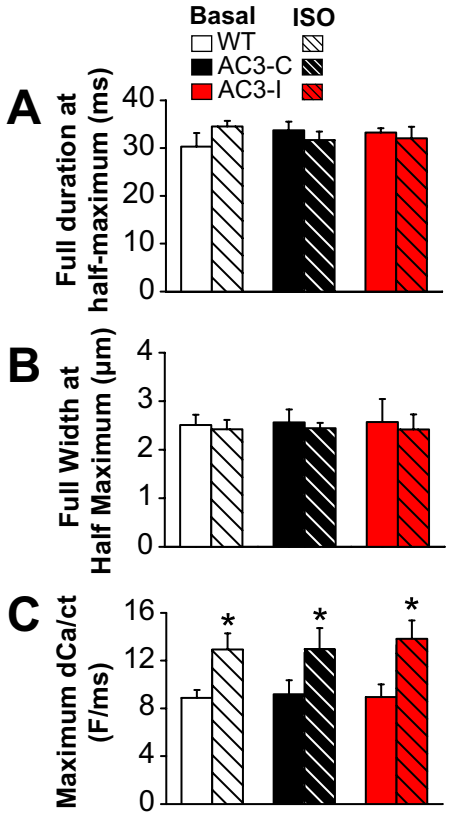

Fig. S5. Similar Ca^{2+} spark kinetics, spatial width, and rate of rise of the intracellular Ca^{2+} transient at baseline and after ISO in AC3-I, AC3-C, and WT SAN cells. (*A*) Ca^{2+} spark durations, measured as the full duration at 50% level of maximum amplitude (FDHM), are not different between genotypes at baseline ($P = 0.8959$) or after ISO ($P = 0.9074$). (*B*) Ca^{2+} spark spatial sizes (FWHM) are also not different between the groups at baseline ($P = 0.988$) or after ISO ($P = 0.997$). (*C*) dCa^{2+}/dt max is not significantly different at baseline ($P = 0.3747$) or after ISO ($P = 0.7260$) between genotypes. dCa^{2+}/dt max increases significantly after ISO in AC3-I ($P = 0.02$), AC3-C ($P = 0.03$), and WT SAN cells ($P = 0.04$).

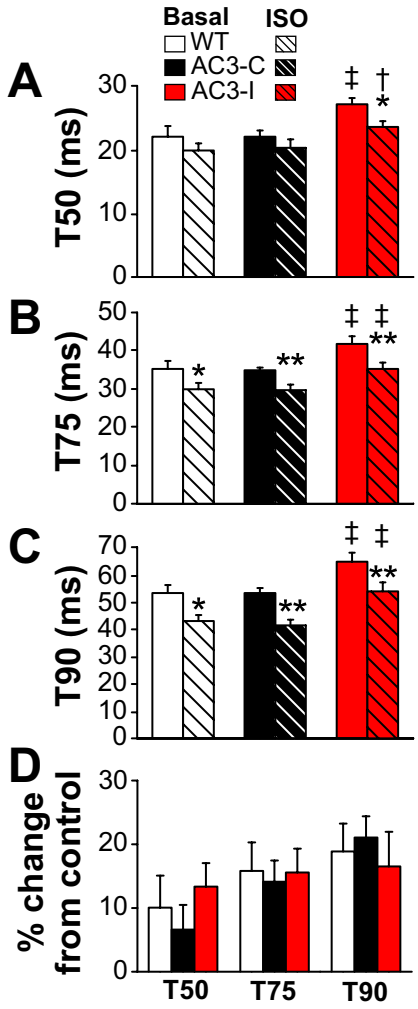

Fig. S6. Slower recovery of the intracellular Ca^{2+} transient in AC3-I compared with AC3-C and WT SAN cells at baseline and after ISO. (*A*) T50 stands for the decay time from peak amplitude to 50% level of the peak Ca^{2+} transient; (*B*) T75 = the decay time from peak to 25% of the peak Ca^{2+} transient; (*C*) T90 = the decay time from peak to 10% of the peak Ca^{2+} transient; (*D*) percent change from control after ISO. *, $P < 0.05$, **, $P < 0.01$ after ISO compared with baseline, †, $P < 0.05$, ‡, $P < 0.01$ AC3-I group compared with control groups.

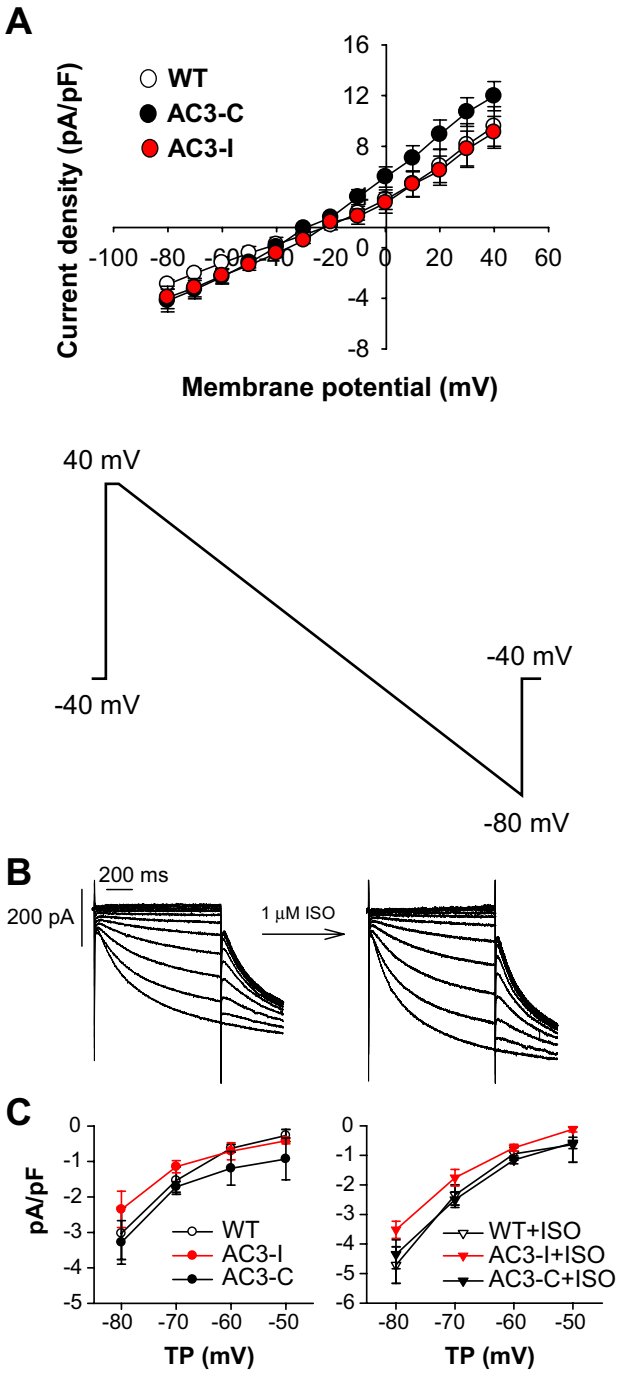

Fig. S7. The I_{NCX} and ''pacemaker'' or ''funny current'' (I_f) are equal in AC3-I, AC3-C, and WT SAN cells. (*A*) No difference in I_{NCX} density between AC3-I, AC3-C, and WT SAN cells. (*Upper*) I_{NCX} current-voltage relationship for $n = 7–9$/data point. (*Lower*) Ramp protocol for I_{NCX} recording. (*B*) A representative recording shows an isoproterenol (ISO) mediated increase in I_f current in a WT SAN cell. (*C*) Summary data show equal I_f density at baseline (*Left*) ($n = 4–8$/group) and after ISO (*Right*) in WT, AC3-C, and AC3-I cells at test potentials (TP) between −50 and −80 mV ($n = 4–8$/group).

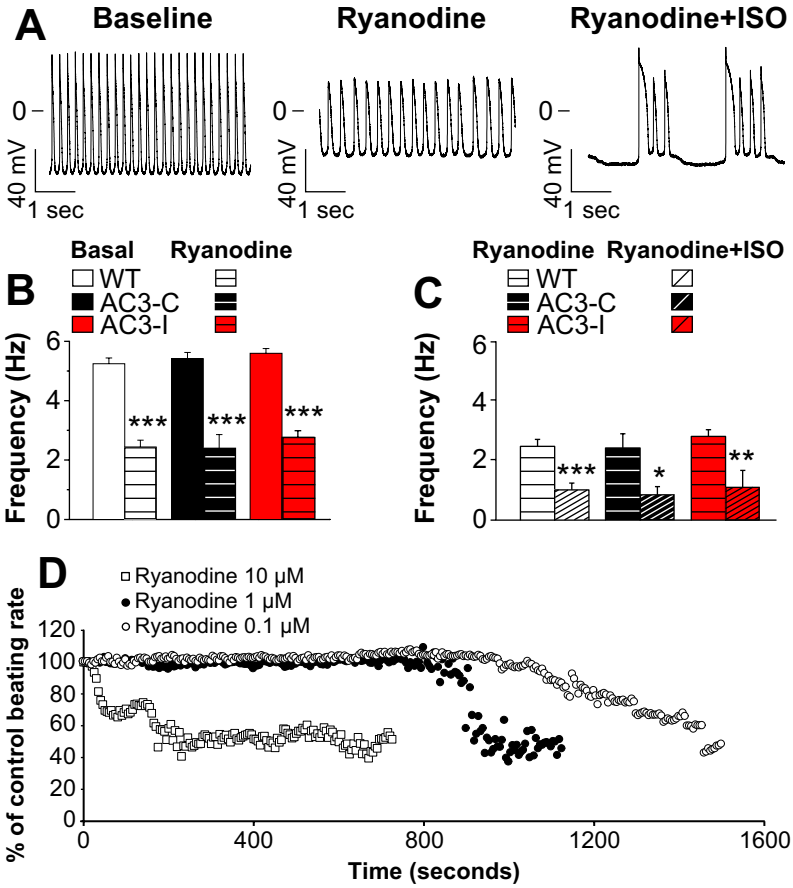

Fig. S8. Ryanodine eliminates differences between AC3-I and control SAN cells. (*A*) Example AP tracings from a WT SAN cell at baseline (left), 35 min after treatment with ryanodine (1 μM, middle) and after addition of ISO (1 μM, right). (*B*) Ryanodine (1 μM) significantly (***, $P < 0.001$) and equivalently slows AP frequencies in AC3-I and control SAN cells ($n = 4$–24/group). (*C*) ISO (1 μM) paradoxically slows AP frequencies in SAN cells after ryanodine. Ryanodine treated SAN cells are the same in (*B*) and (*C*), but only a subset of the ryanodine treated cells are exposed to ISO ($n = 4$–10/group). AP frequencies are not different between AC3-I and control SAN cells after ISO. *, $P < 0.05$, **, $P < 0.01$, ***, $P < 0.001$. (*D*) Concentration and time dependent effects of ryanodine on SAN cell beating rates. Representative recordings of the time course of different concentrations of ryanodine (10 μM, □; 1 μM, ●, and 0.1 μM ○) on SAN cell beating rates. The ryanodine was applied at time 0. Each data point was the mean rate of spontaneous action potentials over 5 sec. Data are normalized to the rate at time 0.

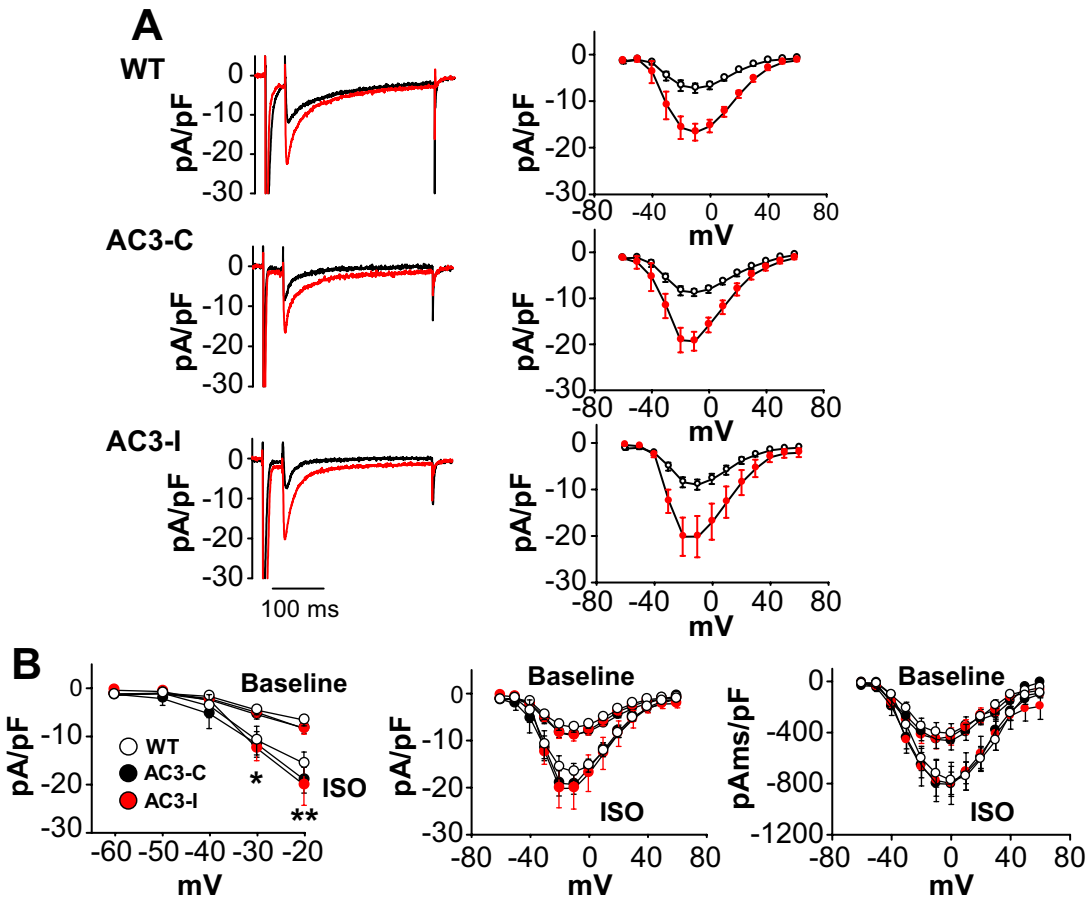

Fig. S9. L-type Ca^{2+} currents in AC3-I, AC3-C and WT SAN cells. (*A*) Representative I_{Ca} current recordings are obtained from WT, AC3-C, and AC3-I SAN cells at baseline (black) and after ISO (1 μM, red), and are paired with complete I-V relationship before and after ISO. (*B*) Summary I-V relationship of I_{Ca} from WT, AC3-C, and AC3-I SAN cells at baseline and after ISO (10–11 cells per group). (*Left*) The I-V at membrane potentials important for phase 4 depolarization (*, $P < 0.05$, **, $P < 0.01$). (*Center*) The complete I-V relationship (peak current density) is shown. (*Right*) The integrated current I-V relationship is shown. Data in *B* are from the cells shown on the *Right* in *A*.